

AperTO - Archivio Istituzionale Open Access dell'Università di Torino

Multi-temporal image co-registration improvement for a better representation and quantification of risky situations: the Belvedere Glacier case study

This is the author's manuscript

Original Citation:

Availability:

This version is available <http://hdl.handle.net/2318/153326> since 2022-06-01T15:06:57Z

Published version:

DOI:10.1080/19475705.2014.927804

Terms of use:

Open Access

Anyone can freely access the full text of works made available as "Open Access". Works made available under a Creative Commons license can be used according to the terms and conditions of said license. Use of all other works requires consent of the right holder (author or publisher) if not exempted from copyright protection by the applicable law.

(Article begins on next page)

This is the author's final version of the contribution published as:

Borgogno Mondino, E., Multi-temporal image co-registration improvement for a better representation and quantification of risky situations: the Belvedere Glacier case study., GEOMATICS, NATURAL HAZARDS & RISK, 6, 5-7,2014,pagg. 362-378, 10.1080/19475705.2014.927804

The publisher's version is available at:

<http://www.tandfonline.com/doi/abs/10.1080/19475705.2014.927804>

When citing, please refer to the published version.

Link to this full text:

<http://hdl.handle.net/2318/153326>

This full text was downloaded from iris-AperTO: <https://iris.unito.it/>

Multi-temporal image co-registration improvement for a better representation and quantification of risky situations: the Belvedere glacier case study

*E. Borgogno Mondino**

DISAFA, Department of Agricultural, Forest and Food Sciences, University of Torino, Grugliasco (TO), Italy.

*Corresponding author. Email: enrico.borgogno@unito.it.

Multi-temporal image co-registration improvement for a better representation and quantification of risky situations: the Belvedere glacier case study

Scientific applications dealing with natural hazards make wide use of digital geographical data and change detection techniques. If the attention is focused on changes affecting surfaces' geometry, multi-temporal aerial photogrammetry can represent an effective tool. In this case the degree of spatial coherence between measurements at different times is an important issue to deal with. Reliability and accuracy of measured differences strictly depend on the strategy used during image processing. In this paper, a simultaneous multi-temporal aerial image bundle adjustment approach (MTBA) is compared against two more traditional strategies for aerial stereo-pairs adjustment to map surface changes of the Belvedere Glacier (Italian North-Western Alps) in the period 2001-2003. Two aerial stereo-pairs (of 2001 and 2003) were used to generate the correspondent digital surface models. These were then compared to map glacier shape differences and calculate ablation and accumulation volumes. Results demonstrate that the proposed MTBA approach improves and maximizes accuracy and reliability of measured differences also when available reference data are low quality ones. Final uncertainty for both direct (surface height differences) and derived (volume changes) measurements were quantified and mapped. Keywords: photogrammetry, aerial bundle adjustment, change detection, glacier dynamics, DSM.

1. Introduction

Geomatics and optical techniques are widely used in the field of damage assessment and risk management related to natural hazards. Olsen et al. (2013) explored limits and potentialities of these techniques particularly focusing on LiDAR and satellite data, stressing the importance of properness of data accuracy and scale respect to the faced application field. They also reviewed change detection techniques reporting some examples concerning natural hazards, showing the important role such approach represents in the natural hazards context. In the specific field of glacier surface change detection, Kääb (2008) made a complete review of geomatics techniques based on

ground and remote approaches stressing the importance of these methods for glaciological studies, especially when glacier dynamics have to be understood over time. Thibert et al. (2005) determined changes in Blanc Glacier (French Alps) comparing DSMs (digital surface models) generated by photogrammetric stereo plotting of aerial images acquired in 1952, 1981, and 2002. Rostom and Hastenrath (1994) assessed the drastic reduction of Mount Kenia glacier generating a DSM from 1993 aerial images and comparing it with height information derived from a 1987 map of the same glacier. More recently Fischer et al. (2011) used DSMs produced by digital aerial photogrammetry (1956, 1988 and 2001) and through airborne LiDAR (2005 and 2007) to investigate the peri-glacial area of the Monte Rosa East Face (Italian Alps).

Kääb (2007) compared a digital elevation model derived from ASTER satellite optical stereo images using photogrammetry with contour lines extracted from a topographic map from the 1970s to measure two small ice caps in Eastern Svalbard, (Kvalpyntfonna and Digerfonna) giving an overall thickness change estimate. Uncertainty in height was measured in the order of 5-10%.

Babu Govindha Raj (2010) measured changes occurred to glacial lakes of Zanskar basin, Jammu and Kashmir (India) in the period 1975-2005 by adopting a change detection approach based on satellite (MSS Landsat-2, TM Landsat-5, ETM+ Landsat-7, LISS III ResourceSat-1) time series. Measurement were then used to estimate the maximum peak lake discharge (m^3/s) which was retained to represent a risky factor. Unfortunately no discussion was made concerning the co-registration level among images nor about the consequent uncertainty of measurements.

Kaufmann et al. (2013) documented glacier retreat in the eastern part of the Granatspitz Mountains (Hohe Tauern Range, Austrian Alps) for the time period 2003-2009 using aerial photogrammetry and 3 aerial acquisitions (2003,2006 and 2009). High resolution

multi-temporal digital elevation models and digital orthoimages of the area of interest were derived for the three periods. Glacier outlines were mapped interactively and compared along the time series demonstrating glaciers retreating. Glacier mass balance was estimated and a mean annual specific net balance amounts was measured.

Gardelle et al. (2011) investigated the evolution of Pamir-Karakoram-Himalaya glaciers giving an estimate of glacier mass balance for 9 study sites spread over the area. The 2000 Shuttle Radar Topography Mission (SRTM) digital elevation model (DEM) was compared with more recent DEMs (2008-2011) derived from SPOT5 stereo imagery observing that during the last decade, the region-wide glacier mass balances suffered from moderate mass losses. Recently Nascetti et al. (2014) tested performance of radargrammetry in generating fast response DSMs in the hydrological risk context. They used COSMO-SkyMed imagery demonstrating that radargrammetry (based on signal amplitude processing) generates better results in terms of accuracy than the more traditional interferometric technique (based on signal phase processing). An interesting feature of this approach is the possibility of georeferencing images without any ground control point performing a sort of image direct georeferencing based on orbital parameter of the satellite itself. No discussion is instead given about uncertainty affecting differences between DSMs generated at different time. Many other works can be found in literature dealing with photogrammetric techniques for DSM generation and comparison along time series. This demonstrates what an important role this technique plays for many scientific applications. Nevertheless it is quite rare to find clear advice about the most efficient and inexpensive method to process data and about the quantification of the final uncertainty of the directly generated products (DEM, DSM, stereo-plotted features, height difference, etc) as well as those derived (areas, volumes, etc). Commonly the focus is on the application, not on the evaluation of the best and

accurate way to obtain expected results. Nevertheless, Käab and Vollmer (2000) suggested the use of simultaneous orientation of multi-temporal images to improve relative accuracy between compared stereo models and their derived products. The same paper suggests the need for stable terrain GCP (ground control points) and inter-annual tie points. Unfortunately no explicit demonstration concerning improvement was given by the simultaneous image orientation approach respect to traditional methods in terms of accuracy. No indication concerning the effect of poor quality GCP was reported as well. Rivera et al. (2005) mapped ice-elevation changes in the period 1975-2001 of the Glaciar Chico, Hielo Patagónico Sur (southern Patagonia ice-field), basing the study on field data, vertical aerial photographs, and satellite images. Concerning aerial photographs, three acquisitions were used (1975, 1981 and 1997) to generate correspondent DSMs, starting from 800 dpi scanned paper prints. Three stereo models were oriented separately and then co-registered with each other. Vertical error was estimated to be about 12 m, from the scale of the original photographs ranging between 1:70,000 and 1:100,000 and the vertical accuracy of GCPs (extracted from existing maps) of about 8.5 m.

Sometimes authors refer to the lack of good quality GCPs (i.e. surveyed by a rigorous ground campaign) when relating to the difficulty of accessing their study area (Rivera et al. 2005), but rarely any indication is given concerning the effect of such limitation. This work tries to partially fill that gap demonstrating that choice of a proper processing workflow can significantly improve final accuracy of measurements and partially overcome limits of poor quality GCPs (ground control points), like the ones extracted from already existing maps (or orthoimages). In particular, the paper shows that the metric uncertainty related to surface change detection can be reduced by simultaneously adjusting all images belonging to the time series. This paper is organized in two parts:

the first one is devoted to investigation of which photogrammetric strategy for multi-temporal aerial images orientation determines the best geometric coherence between DSMs obtained. Relative accuracy affecting DSMs is evaluated with respect to three photogrammetric strategies tested (see section 4): conventional image orientation (BA, bundle adjustment), sequential image orientation (SBA, sequential bundle adjustment) and simultaneous images orientation (MTBA, multi-temporal bundle adjustment). They clearly showed that a MTBA can significantly reduce uncertainty affecting DSMs differences.

In the second part of the paper, results concerning glacier surface change detection are presented. Changes occurring in the period 2001-2003 were mapped by DSM differencing; finally, a demonstration is given of how DSM difference uncertainty propagates along volume calculations.

2. Test site: the Belvedere Glacier

The *Belvedere* glacier is a large, atypical alpine glacier developing along East-face of Monte Rosa mountain (Italian North-Western Alps). It has been being widely studied since the 18th century because of its features that are similar to the ones observable on Himalayan glaciers. First measurements of its area were made by De Saussure (1779-1796) and Amoretti (1817); the high dynamicity of its shape that determined important volume changes (both ablation and accumulation) in the period 1826-1922 was observed and estimated by Monterin (1922) and Fantoli (1928). At that time, the Italian Glaciological Committee had organized topographic and glaciological surveys (Porro & Somigliana 1917, Porro 1917) in the area. During the last twenty years, Belvedere glacier increased the speed of its slide from 35 m/year (1995-1999) to 110 m/year in

1999-2001. It was observed that some parts of the glacier surface lifted up to 30 m, so that the glacier partially overpassed the surrounding moraine.

In 2001 the formation of small peri-glacial lakes began. A year later, in 2002, a wide ephemeral lake formed over the glacier: maximum measured depth was 58 m, and its volume was estimated to be about 3,000,000 m³ (Haeberli et al. 2002). Such a condition generated a risky situation for people living within the municipalities of the Anzasca valley (about 3,500 people), just below the glacier. In fact, a sudden emptying was determined possible due to siphoning or ice avalanches into the ephemeral lake (Humphrey 1987, Diolaiuti et al. 2003, Tamburini et al. 2003). This situation drove the Italian political institutions to use some interventions: thus Italian Civil Protection Corp proceeded to minimally empty the lake lowering the water level about 1 m. Some literature works can be found that deal with the application of remote sensing techniques for Belvedere glacier surface mapping. Noferini et al. (2009) reports about a measurement campaign performed by a ground-based SAR (GB-SAR) in 2007. A glacier DSM was derived by radar interferometry and compared with a topographic map of the area dated 2005 to map occurred changes. Unfortunately unreliable information is given concerning the uncertainty of 2005 reference map and the one of the final SAR measurements, stressing once more the low degree of attention paid by many authors to this basic information.

As far as this work is concerned only the lower part of the glacier is taken into consideration for tests (Fig. 1).

[Fig. 1]

3. Available data

Aerial images

Two aerial stereo-pairs of the glacier were available respectively for the 2001 and 2003 years. During this time period, large movements of the glacier's surface generated great deformations of the surface itself. Table 1 shows the technical features of the original images available.

[Table 1]

Images were supplied as scanned paper prints. Consequently they are very poor quality products, affected by important deformations: partially as a result of their state of conservation, and partially related to the ordinary desktop scanner used to digitize them. The choice of using an ordinary scanner in place of a photogrammetric one was made, once more, to better simulate the worst operational conditions normally related to “quick and dirty” responses. No reliable estimates can be given concerning the first source of deformation, as the state of conservation of printings only depends on conditions that support flatness. On the contrary, some indication can be obtained from literature about deformations introduced by ordinary desktop scanners. Some tests made by Zhu et al. (Zhu et al. 2005), testing performances of UMax Mirage IIse and Microteck commercial scanners, showed that deformations affecting scanned images can range up to 3-4 pixels. Kääh and Vollmer (2000) found that DSMs generated from scanned paper prints (scale 1:6000, 800 dpi, *dots per inch*, scanning resolution) had an accuracy of $\pm 1.7 - 3.5$ m depending on the method used to automatically extract the DSM itself. As far as this work is concerned, images were scanned by an EPSON GT-10000+ scanner at a resolution of 800 dpi corresponding to a physical pixel size of 31.75 μm . According to the average scale of available stereo-pairs mean pixel size at the ground is about 0.65 m for 2001 and about 0.40 m for 2003 images. Consequently, according to Zhu et al. (2005), the scanning step potentially introduced additional image

deformations up to about 2.6 and 1.6 m (4 pixels) respectively for the 2001 and 2003 images. These additional deformations can however be partially absorbed by bundle adjustment. An estimate concerning expected uncertainty of height coordinate (Z) from stereo models can be given according to (1) (Kraus 1993).

$$\sigma_z = \frac{H}{B} \cdot \frac{H}{f} \sigma_x \quad (1)$$

where H is the relative flight height, B is stereo-pair base, f is camera focal length, and σ_x is the accuracy of X parallax measurement (assumed to be equal to half a pixel, i.e. 16 μm). Reference values for height accuracy were reported in Table 1. Cameras calibration certificates were available for internal image orientation.

Reference data

Stereo-pairs were adjusted through LPS bundle adjustment procedures. GCPs were collected in correspondence with stable objects (not changing over time), therefore outside the moving surface of the glacier. The number of GCPs is different depending on the strategy tested and stereo-pair processed. Horizontal coordinates were obtained from an aerial orthoimage, dated 2000, and having a nominal scale of 1:10,000, 1 m resolution, and 2 m horizontal accuracy; GCPs height coordinates were measured from the Digital Elevation Model (DEM) of the Piemonte Region, having a geometric resolution of 50 m and 2.5 m height accuracy. The reference system adopted was WGS84/UTM 32N. These operational conditions naturally determine poorer quality GCPs. This was assumed to be a favorable factor to test the degree to which reference data accuracy can impact relative accuracy between multi-temporal stereo models and which adjustment strategy better minimizes the effect of such uncertainty.

4. Methods

In order to evaluate which bundle adjustment strategy is able to maintain highest possible relative accuracy between multi-temporal DSMs, three approaches were tested: a) single bundle adjustment (BA); b) sequential bundle adjustment (SBA); and, c) multi-temporal bundle adjustment (MTBA). Tests were accomplished using *Leica Photogrammetric Suite 9.1 (LPS)*.

During GCPs identification great attention was paid to ensure that some of them (11) were common to all of the available images (for both years). In addition, for each stereo-pair, some further GCPs were selected to improve bundle adjustment performances at a single time. Finally, 12 Check Points (CHKs), rigorously common to both stereo-pairs, were identified to calculate reference accuracies. For each single stereo-pair some tie points (TPs) were also collected.

Single bundle adjustment (BA)

BA approach can be considered the conventional one: each stereo-pair (2001 and 2003) was adjusted separately and independently using proper GCPs (Fig. 2).

[Fig. 2]

Sequential bundle adjustment (SBA)

SBA is an intermediate approach to achieve bundle adjustment. A stereo-pair is selected as a reference and adjusted using a first set of GCPs. All other stereo-pairs belonging to the time series (for this work, just one), are then adjusted using GCPs extracted (possibly in a stereoscopic way) directly from the already adjusted reference set (Fig. 3). Selection of the reference stereo-pair can be carried out according to two possible criteria. If expectation is to maintain highest possible GCPs accuracy to be identified in

the second step of the process, the reference stereo-pair should be the one acquired at the lowest flight height (that is the most detailed one); if one wants to ensure that GCP for other stereo-pairs adjustment can cover the whole area of each image, the reference stereo-pair is the set having the widest coverage (highest flight height). As identification of GCPs in a mountain area is very difficult (just a few manmade objects exist), the second criterion was adopted for this work and the 2001 stereo-pair was selected as the reference.

[Fig. 3]

Multi-temporal bundle adjustment (MTBA)

This approach simultaneously adjusts all the stereo-pairs of the time series (Fig. 4). The hypothesis was that such operation could improve spatial coherence between oriented stereo models, thus determining a better correspondence between generated DSMs. GCPs used during MTBA were common to all images. As far as TPs are concerned, some preliminary tests carried out (but not presented here) suggested that only TPs linking images of the same stereo-pair can improve adjustment performance; on the contrary, no improvement is obtained using TPs linking images of different stereo-pairs. Moreover, automatic TP detection procedures of LPS did not perform well between images having different scales and different chromatic properties. Further investigation, should be done to explore this issue. TPs were only collected between images belonging to the same stereo-pair. As MTBA uses a single-step adjustment of all images, most of the relative error between different time stereo-pairs (see section 5) is numerically absorbed by the estimates of images' external orientation (EO) parameters.

[Fig. 4]

Figure 5 shows the 2001 and 2003 stereo-pair footprints and distribution of GCPs (triangles) and CHKs (circles); the different scales of stereo-pairs can easily be observed as well as that some GCPs are not common to both stereo-pairs. These were added to better fit each stereo-pair coverage improving adjustment performances. It can also be noted that spatial distribution of GCPs and CHKs appears to be quite irregular. This is a common situation found while working with GCPs and CHKs collected from existing reference datasets, especially in mountain regions where stable points are difficult to recognize and a pre-flight programmed survey is not possible.

[Fig. 5]

Change detection of the Belvedere Glacier surface in the period 2001-2003

According to results from the previous steps, MTBA was applied to orient 2001 and 2003 stereo-models. Consequently two DSMs of the glacier surface were generated through Leica LPS automatic terrain extraction procedure (ATE). The adoption of an automatic point extraction procedure can be considered reasonable as the glacial surface of interest is not affected by shadows nor by vegetation that, usually, represent limiting factors for the performance of dense image matching algorithms. Furthermore, the particular texture of this glacier guarantees that a sufficient number of geometric discontinuities are present as favorable elements in the process. Generated DSMs (grid format) were finally differenced to map changes that had occurred. Height difference uncertainty was set equal to the Z relative accuracy estimated during MTBA. Unreliable areas were identified and mapped over the glacier surface. In these areas it was assumed that measured differences were not significant. This is a very important issue to deal with when deductions must be made to decrease risk.

5. Results

Results show that MTBA improves co-registration of multi-temporal image stereo-pairs and this effect is mainly related to different estimates of image EO parameters. Estimated statistics refer to 12 Check Points and 11 GCPs that are common to all images. The number of TPs is 33 and 41 respectively for the 2003 and 2001 stereo pairs in accordance with the performance of LPS dense image matching processes. All bundle adjustments were performed weighting observations (GCPs) with the declared precision of reference data (2 m for planimetric and 2.5 meters for height coordinates).

Performance comparison of adjustment strategies

As far as this part of the work is concerned, assessment of each strategy compared: a) GCPs/CHKs coordinates (E,N,Z) measured from 2001 and 2003 adjusted stereo-models (*relative accuracy estimate*); b) GCPs/CHKs coordinates (E,N,Z) from each adjusted stereo-model with those from reference datasets (*absolute accuracy estimate*); and, c) differences between image EO parameters obtained through the different adjustment strategies.

Relative accuracy

In this context, relative accuracy is assumed to be equal to the standard deviation of differences (ΔE_i , ΔN_i , ΔZ_i) between CHKs and GCPs coordinates measured from the 2001 and 2003 stereo models (2).

$$\begin{aligned}\Delta E_{i_XBA} &= E_{2003_XBA} - E_{2001_XBA} \\ \Delta N_{i_XBA} &= N_{2003_XBA} - N_{2001_XBA} \\ \Delta Z_{i_XBA} &= Z_{2003_XBA} - Z_{2001_XBA}\end{aligned}\tag{2}$$

XBA is the acronym for the generic bundle adjustment strategy and E, N, Z are the GCP (or CHK) coordinates. Statistics are reported separately for GCPs and CHKs in order to better evaluate adjustment performances. The following statistics were calculated

(Table 2): ΔE , ΔN , ΔZ *mean values*, that can be interpreted as residual systematic (translational) errors after adjustment; ΔE , ΔN , ΔZ *standard deviation values*, that can be interpreted as the residual accidental errors affecting CHKs and GCPs coordinate estimates from models; and, ΔE , ΔN , ΔZ *Root Mean Squared Error (RMSE)*.

[Table 2]

Absolute accuracy

Investigation of the relative accuracy between multi-temporal stereo-pairs does not offer complete information as it does not show how measurements from stereo-models fit reference data. The difference between measured coordinates and reference data is here referred as absolute accuracy. To answer this question, RMSE values for the three spatial coordinates (CHKs and GCPs were jointly considered at this step) were calculated, taking into account differences between measured coordinates and their expected values derived from a reference orthoimage and DEM. Results are shown in Table 3.

[Table 3]

EO parameters differences

In order to complete investigation, the estimated value of EO parameters were compared. Figure 6 shows the differences, respectively, between EO position and attitude parameters.

[Fig. 6]

Change detection of the Belvedere Glacier surface in the 2001-2003 period

MTBA was applied to compute 2001 and 2003 stereo-pairs EO. Two DSMs of the glacier surface (one per year) were generated using Leica LPS ATE procedure. A total of 47,141 (corresponding to a minimum inter-point distance of 1.79 m) and 79,502 points (corresponding to a minimum inter-point distance of 1.49 m) were automatically measured by ATE procedure respectively from 2003 and 2001 stereo models over the glacier surface. Points were successively interpolated by TIN (*Triangulated Irregular Network*) to generate raster DSMs. According to the previously estimated relative accuracy of the E and N coordinates, geometric resolution of DSMs was set to 1 m. DSMs were then differenced to map changes that had occurred (Fig. 7). Uncertainty affecting height difference measurements (HD) was set equal to the estimated standard deviation value (σ_Z) of Table 2 (for CHKs is 1.4 m). Both $1\sigma_Z$ and $2\sigma_Z$ confidence intervals were mapped.

Figure 8 shows areas where differences were unreliable as their values remain outside of confidence intervals ($1\sigma_Z$ and $2\sigma_Z$).

Even excluding these zones, a notable accumulation area can be observed in the front part of the glacier (especially in the two ice tongues). Looking jointly at figures 7 and 8, accumulation of the median part appears not to be significant with respect to the sensibility of measure. An appreciable height decrease, related to the ablation process, is evident in the highest and central median parts of the study area.

[Fig. 7]

[Fig. 8]

Uncertainty concerning Z differences was propagated along volume calculations (Table 4) showing that in the study area (not over the whole glacier) significant volume related to accumulation ranges between about $3.60 \times 10^6 \text{ m}^3$ and about $3.24 \times 10^6 \text{ m}^3$,

depending on the adopted Z confidence interval ($1\sigma_Z$ or $2\sigma_Z$). These estimates reduce accumulation volume estimations of 4.27% and 13.76% respectively. On the other hand, estimates concerning significant ablation volume range between about $3.67 \times 10^6 \text{ m}^3$ and about $3.41 \times 10^6 \text{ m}^3$ depending on the adopted Z confidence interval. In this case, ablation volume reductions were 4.66% and 11.39% for $1\sigma_Z$ and $2\sigma_Z$, respectively.

5. Discussion and Conclusions

Many scientific applications dealing with natural hazards make a wide use of change detection techniques based on remotely sensed data. In particular multi-temporal aerial photogrammetry can represent an effective tool in the hands of specialists. In this paper, starting from a case study concerning the risky situation characterizing the Belvedere glacier, the author was intended to focus on the importance of using some best practices in data management, proving that derived information quality and completeness can be maximized. Moreover this paper demonstrates that good results can be obtained despite having poor quality reference data (GCPs) and that uncertainty of measurements can be effectively used to correctly interpret results. In the final part of the work authors applied previously discussed issues to the case study demonstrating that practical effects of uncertainty are not negligible.

Performed assessments concerning multi-temporal aerial images adjustment demonstrated that, independently from the adopted strategy, the relative accuracy of point coordinates is always higher than the one estimated comparing a reference map with the oriented photogrammetric models; no sum of effects nor error propagation along the Z differences determines relative accuracy of compared DSMs. In fact, the Z differences between single oriented stereo-models and the reference DEM is about 12 m (Table 3) while the lowest relative accuracy between oriented models is about 2.5 m, for the worse performing adjustment method. This is a very encouraging fact for all studies

concerning surface change detection. A further consideration is that relative accuracy is quite independent on the adopted reference data if these remain the same during adjustments. Moreover an appreciable improvement of DSMs relative accuracy can be obtained adopting the MTBA approach. It is worth noting that such improvement is remarkable both for the Z coordinate and for the E and N ones (Table 2). Traditional photogrammetric approach (BA) is always the worse performing; SBA performs satisfactorily for E and N coordinates, but is affected by some systematic errors (mean and standard deviation values are in fact comparable).

Finally, it is not easy to summarize results concerning the estimate of EO parameters obtained using different adjustment strategies. Nevertheless, a sort of asymmetry can be noted from looking at the differences between EO parameters. Fig. 4 shows a higher variability of EO parameters for 2003 images especially. This suggests that the least squares solution (especially for MTBA) operates according to a sort of asymmetric orientation, distributing corrections not equally between stereo-pairs, concentrating them into the 2003 images. This effect could be related to the different scale of images, but further investigations should be done for better understanding.

As far as the case study is concerned some considerations should be done. First of all, it is worth remembering that the Belvedere Glacier (within this paper) merely represents a good, high risk example which would benefit from the adoption of the suggested methodology both in terms of data processing and interpretation of results. It was not the intention of the author to give a complete and comprehensive technical description of the actual situation of the area, but rather to invite, through this example, once more, the operative scientific and technical community to manage available geographical data (and in particular the photogrammetric data) diligently. Many potentialities can be found in low quality data, but an improper reading may involve many

misunderstandings. Some interesting technical information can be derived from this application of MTBA to the Belvedere case study. In fact, as Haeberli et al. (2002) found, DSMs difference mapping shows a strong lift of the final part of the glacier. Accumulation in the lower glacier and ablation in the upper part confirms this trend and suggest that the glacier was not affected by an ordinary supply of material coming from the nearby slopes, but that it suffered from an anomalous mass transfer downward with respect to the valley. Further deductions can be made concerning the size of areas and volumes mainly involved in surface dynamics which value varies with height difference uncertainty and its propagation along volume computation. In a natural hazard context, like the one explored here, this is a very important issue as ice volume can be directly related to potential amount of flooding water threatening the local population. Engineers and technician, opportunely informed about this value, can more properly make decisions. Furthermore, the possibility of distinguishing and mapping significant and not-significant height differences permits a better interpretation of the glacier's dynamics and helps to better focus on the proper and riskier parts of the glacier. From this point of view, both volumes and areas that more reliably suffer from changes are considerably lower than those that can be obtained through direct computation from all the mapped Z differences (Table 4). This additional information can drive to different interpretations and better inform actions of decision makers.

7. Acknowledgements

Acknowledgements are due to Peter Schlesinger for the linguistic revision and to Dr. G. Mortara, Geom. F. Godone of the Italian Research National Council – IRPI of Torino, Dr. A. Tamburini and Dr. D. Godone for supplying part of the reference bibliography concerning the Belvedere Glacier and the aerial paper prints.

References

Amoretti. 1817. *Viaggio da Milano ai tre laghi Maggiore, di Lugano e di Como e ne' monti che li circondano*. [Travel from Milan to the three lakes Maggiore, of Lugano and of Como and within surrounding mountains]. Giuseppe Galeazzi, Milano (I), Italian.

ARPA Piemonte. 2002. *Il lago epiglaciale del ghiacciaio del Belvedere a Macugnaga*.

[The Belvedere glacier epi-glacial lake in Macugnaga]. Italian. Available from: <http://www.arpa.piemonte.it/pubblicazioni-2/relazioni-tecniche/analisi-eventi/eventi-2004/pdf-macugnaga/atdownload/file>.

Babu Govindha Raj, K. 2010. Remote sensing based hazard assessment of glacial lakes: a case study in Zaskar basin, Jammu and Kashmir, India. *Geomatics, Natural Hazards and Risk*, 1:4, 339-347.

De Saussure H. B., 1779-1796. *Voyage dans les Alps*. [Travel within Alps]. Franch. Vol. 4, p. 348. Société typographique de Neuchâtel, Neuchatel (CH).

Diolaiuti G., D'Agata C., Smiraglia C. 2003. Belvedere Glacier. Monte Rosa, Italian Alps: tongue thickness and volume variations in the second half of the 20th century. *Arctic, Antarctic and Alpine Research*. 35:255-263.

Fantoli A. 1928. *I laghi glaciali e gli impianti alpini*. [Glacial lakes and alpine plants]. *L'energia elettrica*, anno 6, vol. 5 (2), p. 230.

Fischer, L., Eisenbeiss, H., Käab, A., Huggel, C., Haeberli, W. Monitoring topographic changes in a periglacial high-mountain face using high-resolution DTMs, Monte Rosa East Face, Italian Alps. *Permafrost and Periglacial Processes*, 22/2: 140-152.

Gardelle, J., Berthier, E., Arnaud, Y. & Käab, A. 2013. Region-wide glacier mass balances over the Pamir-Karakoram-Himalaya during 1999–2011. *Cryosphere*, vol. 7, no. 4, pp. 1263-1286.

Haeberli W., A. Käab, F. Paul, M. Chiarle, G. Mortara, A. Mazza, P. Deline and S. Richardson. 2002. A surge-type movement at Ghiacciaio del Belvedere and a developing slope instability in the east face of Monte Rosa, Macugnaga, Italian Alps. *Norwegian Journal of Geography*. 56:104-111.

Humphrey N. F. 1987. *Basal Hydrology of a Surge-Type Glacier: Observations and Theory Relating to Variegated Glacier*. [dissertation]. Seattle: University of Washington, 1987.

Käab, A. 2007. Glacier volume changes using ASTER optical stereo. A test study in Eastern Svalbard. *International Geoscience and Remote Sensing Symposium (IGARSS)*, pp. 3994.

Käab, A. 2008. Remote sensing of permafrost-related problems and hazards. *Permafrost and Periglacial Processes*, 19, 107-136

Käab, A., & Vollmer, M. 2000. Surface geometry, thickness changes and flow fields on creeping mountain permafrost: Automatic extraction by digital image analysis. *Permafrost and Periglacial Processes*, 11, 315-326

Kraus, K. 1993. *Photogrammetry*. Ferdinand Dummlers Verlag, Bonn (Germany).

Macaluso, G., Pieraccini, M., & Atzeni, C. 2009. Monitoring of Belvedere Glacier using a wide angle GB-SAR interferometer. *Journal of Applied Geophysics*, 68, 289-293.

Monterin U. 1922. The Macugnaga glacier from 1780 to 1922. *Bollettino del Comitato Glaciologico Italiano, Società Italiana per il Progresso delle Scienze, Roma*. 5:12-40. Italian.

Nascetti, A., Capaldo P., Porfiri M., Pieralice F., Fratarcangeli F., Benenati L., Crespi M. 2014. "Fast terrain modelling for hydrogeological risk mapping and emergency

management: the contribution of high-resolution satellite SAR imagery." *Geomatics, Natural Hazards and Risk*: 1-30.

Noferini, L., Mecatti, D., Kaufmann, V., Plösch, R., Ritter, S. & Streber, J. 2013. Documentation of the glacier retreat in the eastern part of the Granatspitz Mountains (Austrian Alps) using aerial photographs for the time period 2003-2009. *Cartographic Journal*, vol. 50, no. 3, pp. 232-239.

Olsen, MJ., Chen, Z., Hutchinson, T., Kuester, F. 2013. Optical techniques for multiscale damage assessment. *Geomatics, Natural Hazards and Risk*, 4 (1), 49-70.

Rivera, A., Casassa, G., Bamber, J., & Kääb, A. 2005. Ice-elevation changes of Glaciar Chico, southern Patagonia, using ASTER DEMs, aerial photographs and GPS data. *Journal of Glaciology*, 51, 105-112

Rostom R.S., Hastenrath S. 1994. Variations of Mount Kenya's glaciers 1987-1993. *Erdkunde*, 48:174-180.

Tamburini A., Mortara G., Belotti M., Federici P. 2003. The emergency caused by the "Short-lived Lake" of the Belvedere Glacier in the summer 2002 (Macugnaga, Monte Rosa, Italy). *Studies, survey techniques and main results. Terra Glacialis* 6:37-54.

Thibert E., Faure J., Vincent C. 2005. Mass balances of the Glacier Blanc between 1952, 1981, and 2002 calculated from digital elevation models. *Houille Blanche*. 2:72-78.

Zhu, H., Scarpace, F.L., & Stevens, M. 2005. Correcting Geometric Errors From Desktop Scanners. In, *ASPRS 2005 Annual Conference : "Geospatial Goes Global: From Your Neighborhood to the Whole Planet"*. Baltimore, Maryland: ASPRS

Wangensteen, B., Gudmundsson, Á., Eiken, T., Kääb, A., Farbro, H. & Eitzelmüller, B. 2006. Surface displacements and surface age estimates for creeping slope landforms in

Northern and Eastern Iceland using digital photogrammetry, *Geomorphology*, vol. 80,
no. 1-2, pp. 59-79.

Figures

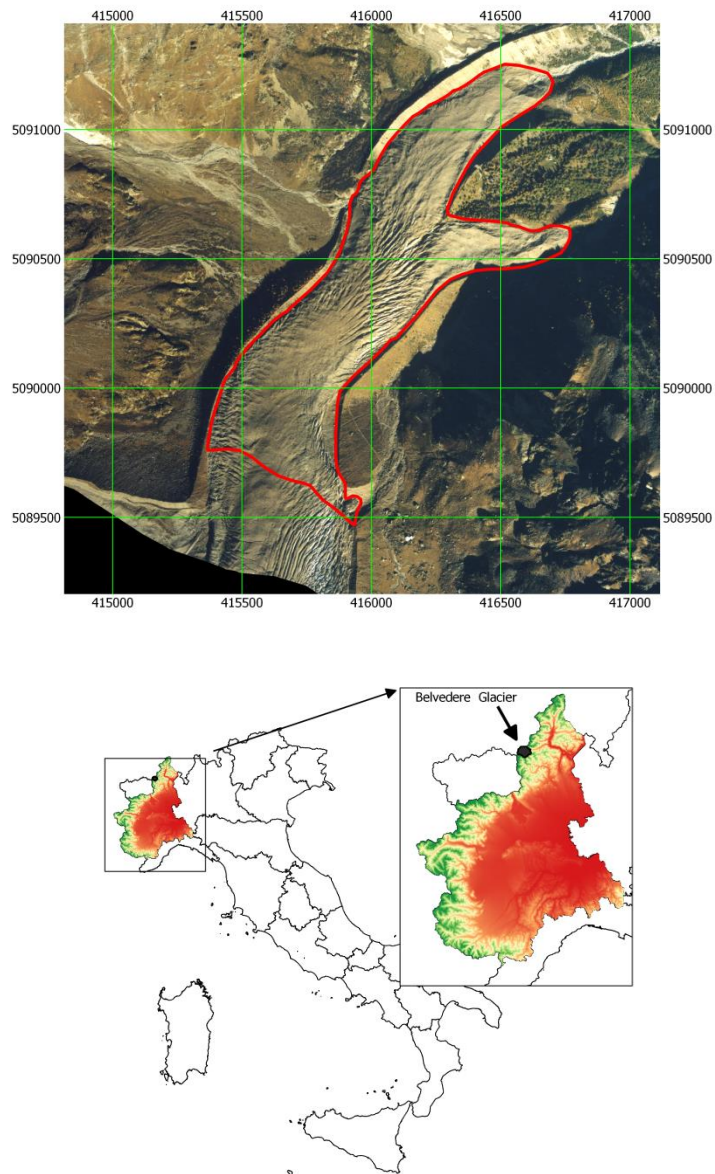


Fig. 1. Orthoimage of Belvedere Glacier. Investigated area is the red one (above). Belvedere Glacier position (in black) respect to Piemonte region (colored area) and Italy (below).

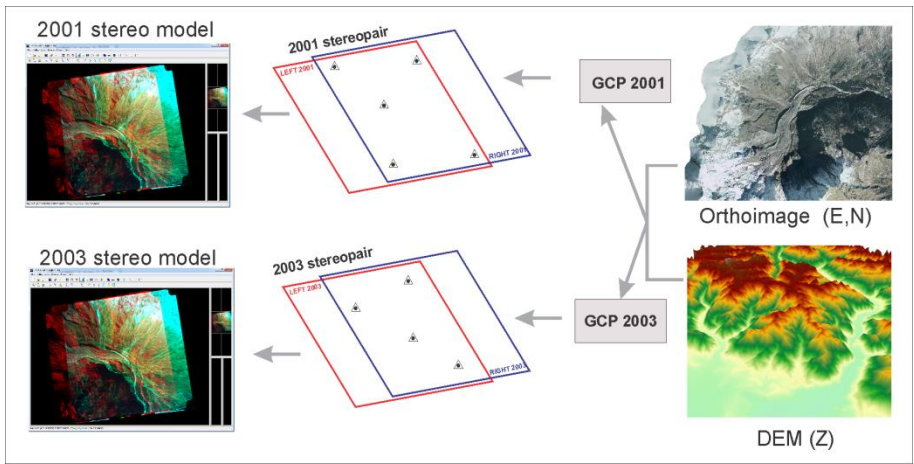


Fig. 2. Single Bundle Adjustment (BA) flow chart.

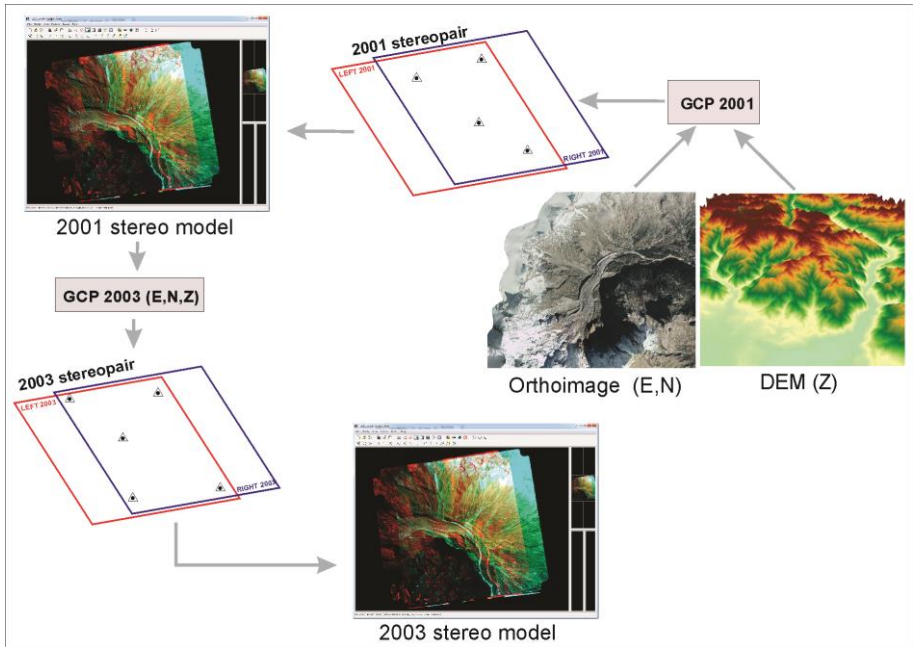


Fig. 3. Sequential Bundle Adjustment (SBA) flow chart.

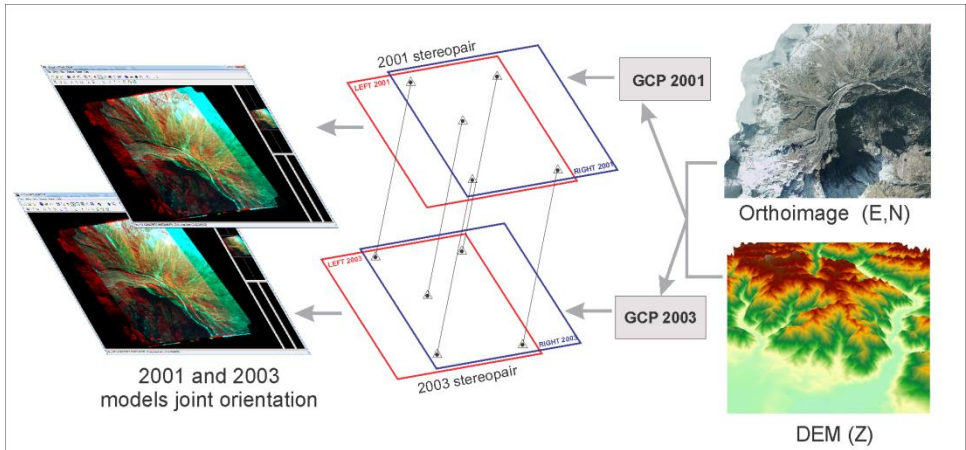


Fig. 4. Multi-Temporal Bundle Adjustment (MTBA) flow chart.

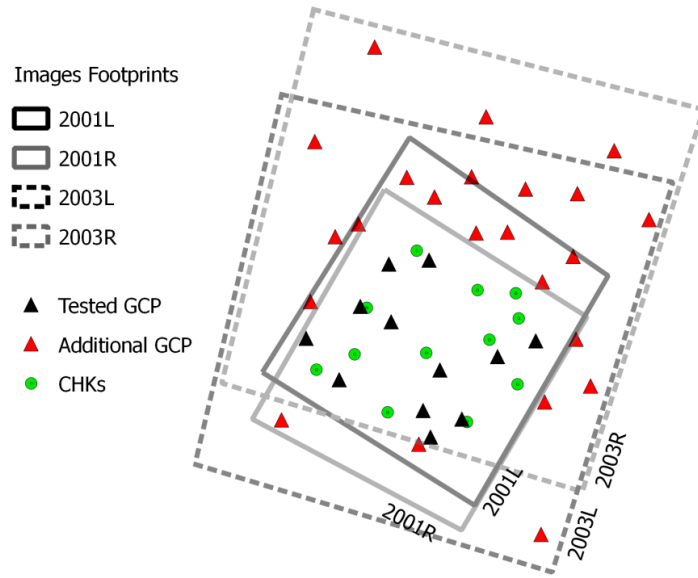
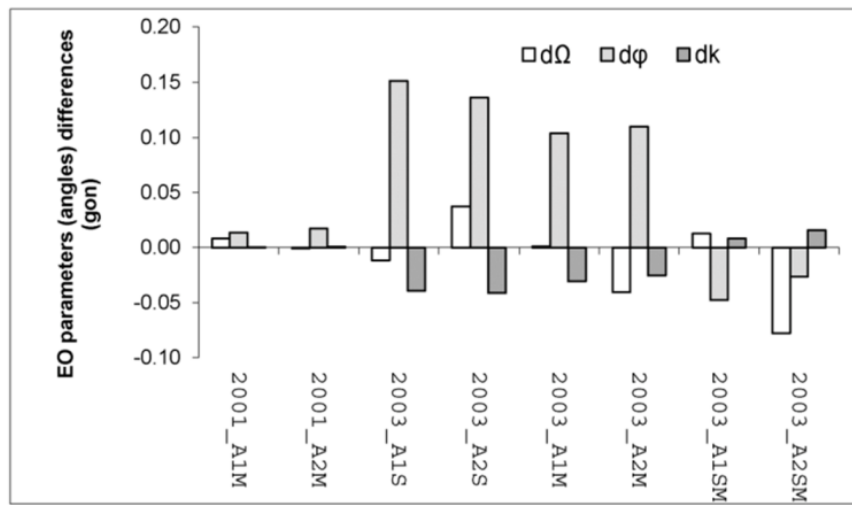
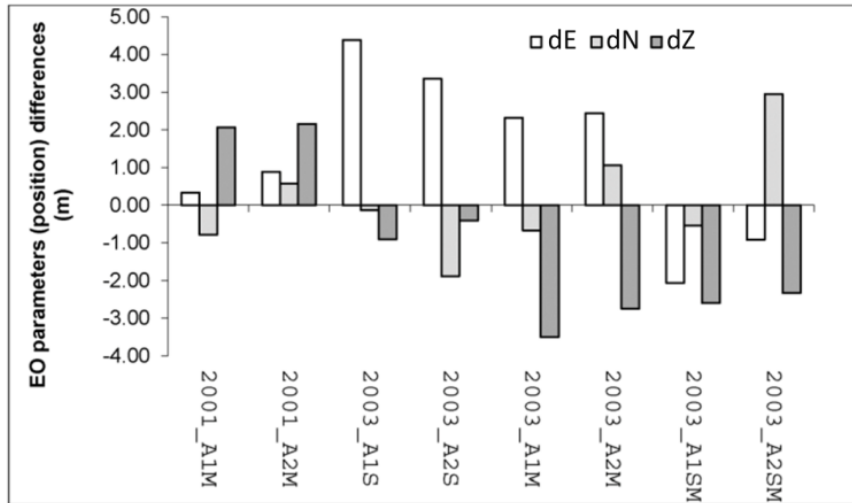


Fig. 5. 2001 and 2003 image footprints after adjustment (MTBA solution); *Triangles* = GCPs (in black those common to both images); *Circles* = CHKs.



Label	Definition
2001_A1M 2001_A2M 2003_A1M 2003_A2M	Differences concerning EO parameters values estimated respectively through BA and MTBA (A1, A2 are images belonging to the same stereo-pair).
2003_A1S 2003_A2S	Differences concerning EO parameters values estimated respectively through BA and SBA. 2001 stereo-pair is the reference one for SBA.
2003_A1SM 2003_A2SM	Differences concerning EO parameters values estimated respectively through SBA and MTBA.

Fig. 6 – Graphs showing differences of EO parameters values obtained through the three tested adjustment strategies.

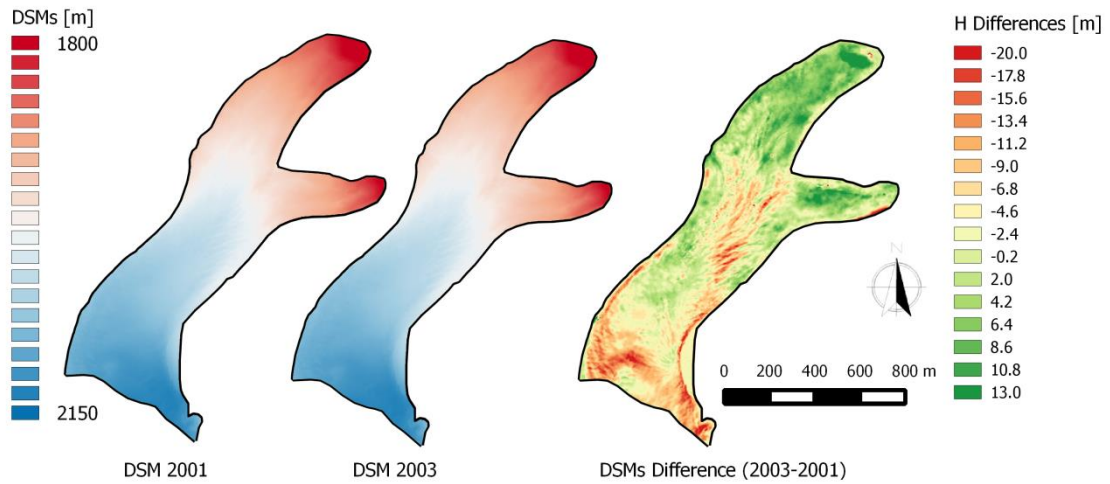


Fig. 7. 2001 and 2003 DSMs and Height difference map showing glacier surface changes occurring in the period 2003-2001.

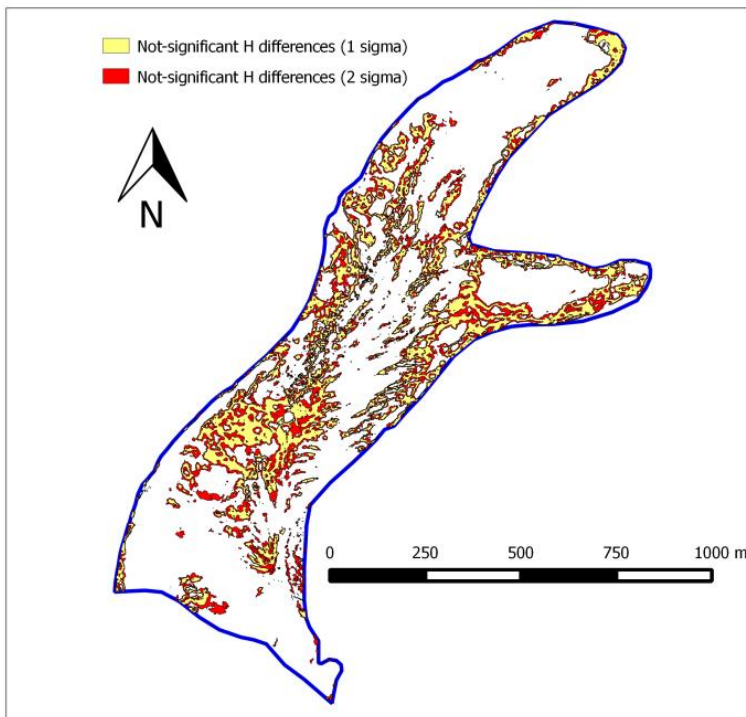


Fig. 8. Map showing areas where surface changes were considered unreliable. The yellow areas show where height differences are lower than $\pm 1\sigma_z$, whereas, red areas show where height differences are lower than $2\sigma_z$.

Tables

Stereo-pair	Image mean scale	Relative Flight Height (H)	Base (B)	Calibrated Focal Length	Theoretical σ_z
2001	$\approx 1 : 20,000$	$\approx 3,000$ m	≈ 750 m	151.946 mm	≈ 1.5 m
2003	$\approx 1 : 12,000$	$\approx 1,750$ m	≈ 550 m	152.815 mm	≈ 0.6 m
Camera type				Lens number	Date of calibration
2001	WILD RC5 15/4 UAG			407	December 16, 2000
2003	WILS RC20 15/4 UAGA-F			13128	January 1, 2000

Table 1. Technical data concerning available aerial stereo-pairs.

	ΔE (m)			ΔN (m)			ΔZ (m)		
	BA	MTBA	SBA	BA	MTBA	SBA	BA	MTBA	SBA
CHK mean	-0.57	-0.09	0.50	-0.25	0.05	0.43	-1.44	0.21	1.77
CHK std dev	1.55	0.74	0.64	1.74	0.98	0.77	2.13	1.40	1.97
CHK RMSE	1.66	0.75	0.79	1.76	0.98	0.85	2.61	1.42	2.58
GCP mean	-0.66	0.09	0.83	-0.38	-0.14	0.65	0.30	0.10	1.81
GCP std dev	2.19	0.29	0.67	2.00	0.33	0.86	2.61	0.64	2.06
GCP RMSE	2.30	0.31	1.03	2.04	0.36	1.03	2.63	0.65	2.71

Table 2. Statistics concerning relative accuracy. Differences refer to E, N and Z coordinate values from 2001 and 2003 multi-temporal oriented stereo models (adjusted by different strategies).

	2003	2001	2003	2001	2003 over 2001
	BA	BA	MTBA	MTBA	SBA
RMSE E [m]	2.99	1.87	2.27	2.00	3.08
RMSE N [m]	1.90	1.90	1.81	1.77	2.07
RMSE Z [m]	12.13	12.23	12.08	12.31	12.82

Table 3. Absolute accuracy. RMSE of E, N and Z coordinates computed with respect to reference data.

		Area [ha]	Volume [m ³]	Volume uncertainty [m ³]	Volume uncertainty [%]
Ablation	1 σ	30.7	3.66917 x 10 ⁶	179,420	4.66
	2 σ	(37.1)	(3.41013 x 10 ⁶)	(438,460)	(11.39)
Accumulation	1 σ	27.34	3.59859 x 10 ⁶	160,400	4.27
	2 σ	(21.81)	(3.24173 x 10 ⁶)	(517,260)	(13.76)

Table 4. Surface and volume values (ablation and accumulation) and related uncertainty (1 σ and 2 σ) for the study area.